

CHAPTER 1

INTRODUCTION

The early history of proton transport

Exactly 200 years ago this year Theodore von Grotthuss, at the fresh age of 21, deduced the primary elements of the ‘excess’ proton’s unique mode of diffusion in water. With his seminal 1806 publication of “Sur la décomposition de l'eau et des corps qu'elle tient en dissolution à l'aide de l'électricité galvanique”¹ Grotthuss not only correctly discerned the existence and nature of the water molecule’s electric dipole, but outlined the ‘bucket line’ like process wherein a hydrogen atom is transported through an exchanged between the oxygen atoms in a line of water molecules; particularly remarkable considering the limited understanding of the composition of matter.

Grotthuss’ 1806 publication appeared in the newly created (and soon to fail) *Annales de Chimie*, a publication founded by the father of modern chemistry, Antoine-Laurent Lavoisier. Only a year prior to Grotthuss’ publication John Dalton had presented a series of papers to the Literary and Philosophical Society of Manchester, in which he outlined the key points of his atomic theory of matter. Five years later Dalton would publish *A New System of Chemical Philosophy*² firmly establishing his fully developed atomic theory of matter.

Grotthuss formulated the fundamental mechanism of proton transport during the genesis of chemistry as a science, and still we lack a detailed and comprehensive picture of proton solvation and transport. The early foundation and the significance of the remaining questions are a testament to the challenging subtleties of this problem.

Molecular dynamics briefing

Molecular dynamics (MD) is simply the modeling of the dynamical behavior of atoms and molecules with a computer. The dynamical evolution of the atoms in a MD simulation is accomplished by numerically integrating their equations of motions. Forces on the atoms are calculated from the potential energy function of the model, which varies parametrically with the atomic coordinates. From the forces on a given atom, Newton's first law and some computationally convenient variations of the kinematic equations of motion can be used to propagate the atomic coordinates over an appropriately short time interval.

The following discussion is a very brief overview of the methods and common practices used in MD simulations. A more complete discussion, including the implementation, subtleties, method limitations, and so forth, can be found in Ciccotti and Hoover,³ Allen and Tildesley,⁴ Haile,⁵ or Rapaport.⁶

The potential

The potential, or equally model or force field, is frequently written as a sum of pair-wise interactions,

$$V(r_1 \dots) = \sum_{ij}^{all\ pairs} f(|r_i - r_j|). \quad 1.1$$

The forces for a particular atom are then calculated as the gradients of the atomic displacements,

$$F_i = -\nabla_{r_i} V(r_1 \dots). \quad 1.2$$

It should be noted that this two-body potential form poorly approximates many interactions and consequently various many body potentials are commonly used for the

relevant systems. Additionally, purely empirical potentials can be discarded in favor of solving the electronic structure problem, so-called *ab initio* MD. This is currently only feasible for short and relatively small simulations using severe approximations to solve for the electronic degrees of freedom. The work contained in this thesis exclusively uses the pair-wise potential form.

Whatever the functional form of the potential, it is only practical to calculate the interactions of atomic pairs for only relatively small clusters of atoms or molecules. To effectively simulate bulk-like systems it is necessary to truncate the potential to reduce the intractable number of interacting pairs at long distances. The manner of truncation is critical. It should avoid severe discontinuities that spoil energy conservation, as well as accounting for changes in the systems' cohesive energy or total pressure. Treatment of long-range potential forms, like electrostatic potentials, is especially difficult and requires particular considerations at the cutoff and boundaries of the system.

Boundary conditions

Given that bulk-like simulations that explicitly include all atoms in a system are currently intractable, one solution is to simulate a manageable number of atoms or molecules and simply replicate them periodically in all directions to infinity. The potential cutoff is then chosen with deference to the dimensions of the system. When the cutoff is less than half of the systems shortest dimension, a given atom interacts with only the nearest image of all other atoms; the so-called minimum image convention.

In the event that an atom crosses a boundary, it is inserted into the system at the opposite boundary with the same displacement and velocity. In this manner, a fully

deterministic trajectory can be constructed for each unique atom in the system. From these trajectories it is then possible to relate the long time averaged atomic properties to macroscopic thermodynamic properties.

Statistical mechanical ensemble

Molecular dynamics is a statistical mechanical method. It is used to construct atomic and molecular trajectories from which a set of configurations distributed according to a statistical distribution, or equally, a statistical ensemble, are collected. The property of interest is then averaged over all these configurations. This is a central assumption of statistical mechanics; the long time average of the observed property is equivalent to the ensemble average. It is implicitly assumed that during a measurement all possible states are visited, and that the observed properties are simply the averages from these states. This is the connection between the microscopic behavior (the simulation) and thermodynamics.

The multistate empirical valence bond method

Protons in liquid water exhibit an anomalously large mobility relative to other simple monovalent cations.⁷ This unusual mobility has been attributed to the Grotthuss mechanism, wherein the charge defect associated with the excess proton is passed from one water molecule to another through fluctuating covalent and hydrogen bonds; Figure 1.1.

The basic structural mechanism first proposed by Grotthuss has subsequently been refined, supposing translocation occurs through the interchange between two

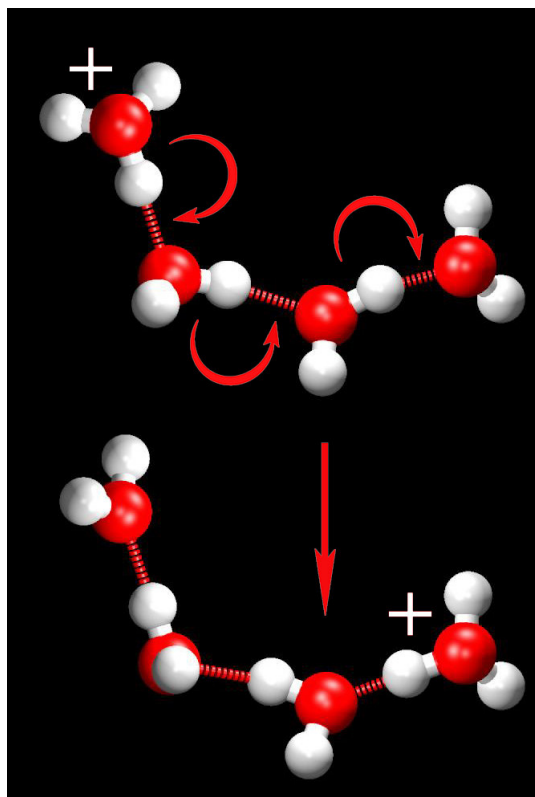


Figure 1.1. The fluctuating bonding topology of the Grotthuss mechanism. Hydrogen bonds (thin, broken) are replaced with covalent bonds (thick, solid), and likewise covalent bonds are replaced with hydrogen bonds. The charge defect can be conveyed through several water molecules without significant nuclear rearrangement.

distinct solvation structures. Eigen proposed that the hydronium cation (H_3O^+) was strongly solvated by three water molecules, which will hereafter be referred to as the Eigen cation or Eigen structure (H_9O_4^+ , Figure 1.2.a).⁸ Zundel speculated that the excess proton was solvated more or less equally by two water molecules, hereafter referred to as the Zundel cation or Zundel structure (H_5O_2^+ , Figure 1.2.b).⁹

Modeling the interplay between these limiting structures, or more completely, the dynamical bonding topology evolving along a potential energy surface (PES) is a significant challenge. Traditional classical MD force fields are generally incapable of treating this fluctuating bonding topology.

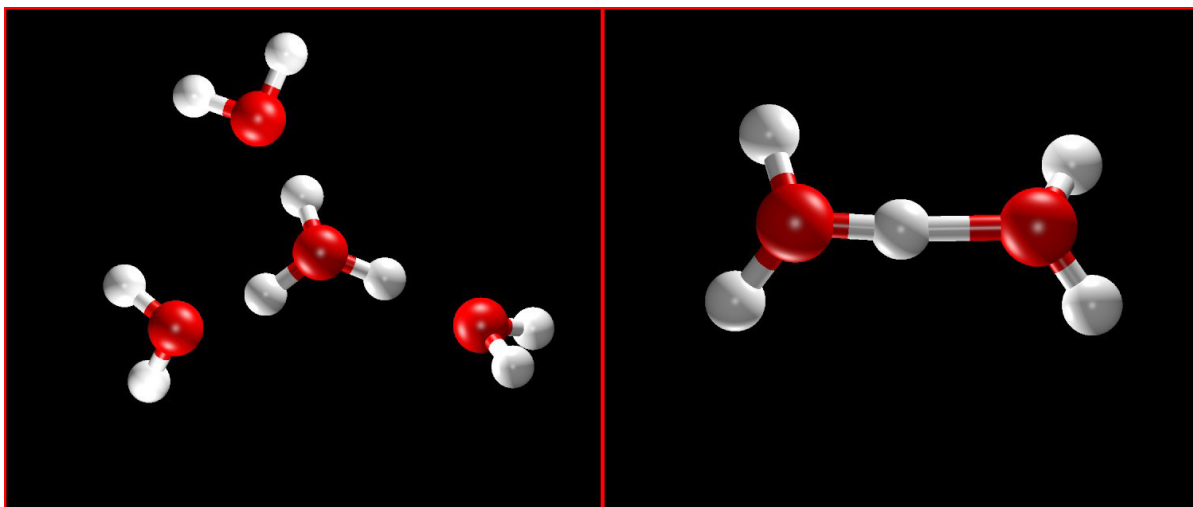


Figure 1.2. Panel a, left: The solvation structure proposed by Eigen. Panel b, right: The solvation structure proposed by Zundel.

However, the multistate empirical valence bond (MS-EVB) method, which is described below, has proven capable of modeling the evolving bonding topology of explicit proton transport within the framework of a traditional MD simulation. Moreover, the method lends itself to the construction of a proton transfer PES custom fit to surfaces calculated from exceedingly accurate electronic structure methods.^{10,11}

MS-EVB

The empirical valence bond (EVB) method was first formulated by Warshel¹² by extending the valence bond schemes of Mulliken¹³ and Coulson.¹⁴ Warshel's EVB method was first applied to the problem of proton transport through a simple two state model by Lobaugh¹⁵ and later extended to a many state treatment by Schmitt.¹⁶ And, although the MS-EVB model has been through several subsequent parameter refinements, throughout the implementation has remained consistent.¹⁶⁻¹⁸

The MS-EVB method supposes that the PES for the aqueous excess proton can be constructed as a linear combination of the potential expressions for a set of limiting bonding topologies. Take, as an example, the solvated proton and the associated collection of water molecules in Figure 1.3. The bonding topology can be arranged in a large number of configurations for all possible $\text{H}_2\text{O}/\text{H}_3\text{O}^+$ permutations. However, most of these combinations can be ruled out due to the unlikely bond lengths and angles. The choice of contributing states is empirically motivated.

With the collection of states in hand, the global PES is constructed from the potential for each state. Assuming orthogonality among the basis states, the Hamiltonian is then written such that,

$$\langle i | H | i \rangle = V_{\text{H}_3\text{O}^+}^{\text{intra}} + \sum_k^{N_{\text{H}_2\text{O}}} V_{\text{H}_2\text{O}}^{\text{intra},k} + \sum_k^{N_{\text{H}_2\text{O}}} V_{\text{H}_3\text{O}^+, \text{H}_2\text{O}}^{\text{inter},k} + \sum_{k < k'}^{N_{\text{H}_2\text{O}}} V_{\text{H}_2\text{O}}^{\text{inter},kk'}, \quad 1.3$$

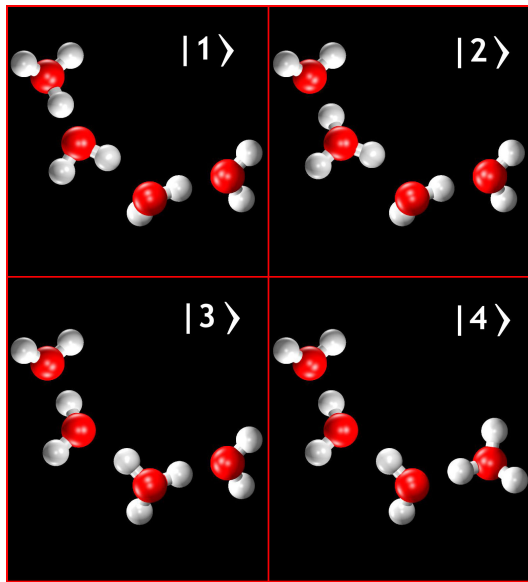


Figure 1.3. The empirically motivated states used to construct the MS-EVB potential.

a sum of hydronium intramolecular, water intramolecular, and hydronium-water and water-water intermolecular interactions respectively. The off diagonal terms,

$$\langle i | H | j \rangle = (V_{const}^{ij} + V_{exchange}^{ij}) A(R_{OO}, R_{OH}), \quad 1.4$$

are a function of constant and exchange electrostatic terms varied by a geometric dependent function. Each element $h_{ij}(\mathbf{x})$ of \mathbf{H} is a function of the nuclear degrees of freedom \mathbf{x} of the collection of atoms.

The diagonal terms have a fairly simple dependence on the nuclear degrees of freedom and are represented by previously validated force fields, effectively fixing the asymptotes of the proton transfer reaction. The off diagonal functional form and parameters are chosen to accurately reproduce the electronic structure PES coupling the reacting species described by the diagonal elements. The exact functional form and parameter values have been tabulated by Day et al.¹⁷ and the references therein.

From the Hamiltonian, the ground-state eigenvector is calculated and the forces are found using the generalized Hellmann-Feynman theorem,

$$F_i = -\langle \Psi_0 | \frac{\partial H}{\partial x_i} | \Psi_0 \rangle = -\sum_{m,n} c_m^0 c_n^0 \frac{\partial}{\partial x_i} h_{mn}(x). \quad 1.5$$

With the forces it is now possible to propagate the nuclear coordinates constructing a trajectory; the nuclear coordinates are updated, a new force calculation is performed, and the process is repeated.

SCI-MS-EVB

A straightforward extension of the MS-EVB method to an aqueous solution of more than just a few excess protons results in an intractably large number of states. A matrix constructed as the product basis set of all excess protons would be of the order of

N^m , where N is the number of basis states accessible to each excess proton and m is the number of excess protons. In a bulk water MS-EVB simulation the enumerated states are restricted to the first three proton solvation shells, so N would typically fluctuate between 20 to 30 states. For two excess protons the order of the Hamiltonian would be greater than 15,000, for three it would exceed 390,000. The necessary repeated solution for a trajectory of any reasonable length with this number of states is currently computationally infeasible.

One solution is to initially treat each excess proton independently of all others. Several single proton ‘EVB complexes’ are constructed by dividing the system into groups containing an excess proton and some number of associated solvating water molecules. The self-consistent iterative multistate empirical valence bond (SCI-MS-EVB) method, developed by Wang et al.,¹⁹ iteratively solves these single proton eigenvalue problems within the effective field of all other EVB complexes. This effective field represents the interactions between EVB complexes and the remaining atoms through interaction parameters scaled by the state populations of the corresponding EVB complex.

Consider a two-proton system with EVB complex A and B. The single proton EVB complex Hamiltonian is written, as it would be in the MS-EVB method, according to equations 1.3 and 1.4. The Hamiltonian for complex A is then partitioned into contributions from interactions between those atoms within the complex, H_{AA} , interactions between atoms in complex B and those in complex A, H_{AB} , and interactions between atoms in complex A and those not in any EVB complex, H_{AR} . The Hamiltonian for complex A is then,

$$H_A = H_{AA} + H_{AB} + H_{AR}. \quad 1.6$$

Note that the same expression for complex B also contains H_{AB} , that is, $H_{AB}=H_{BA}$. The solution for either depends simultaneously on the solutions for both complex A and B.

In general, the effective parameters for any interaction are then defined as the population weighted sum of the parameters from the potential energy expressions used to construct the Hamiltonian. For example, the van der Waals interaction parameter,

$$\alpha = (4\epsilon)^{1/12} \sigma, \quad 1.7$$

is written as,

$$\alpha_s = c_{Bi}^2 \alpha_{sH} + \sum_{i \neq j} c_{Bj}^2 \alpha_{sW}, \quad 1.8$$

for the effective particle s in complex B such that α_{sH} and α_{sW} are the van der Waals parameters for particle s in either a hydronium molecule or water molecule respectively with EVB coefficients c_{Bi} and c_{Bj} for states i and j. Once a convergent self-consistent solution is found, the generalized Hellmann-Feynman theorem is used to find the forces from the energy expression,

$$E_{total} = \langle a_0 | H_{AA} + H_{AR} | a_0 \rangle + \langle b_0 | H_{BB} + H_{BR} | b_0 \rangle + \langle a_0 b_0 | H_{AB} | a_0 b_0 \rangle + E_{RR}. \quad 1.9$$

The above procedure supposes distinct and separable EVB complexes. So, what then is to be done with those regions where two EVB complexes share common water molecules? The method can be extended to explicitly treat these water molecules. However, in doing so we would find that this common water molecule would be doubly protonated with probability $c_{Ai}^2 c_{Bi}^2$. A state with substantial values for both coefficients would certainly be a high-energy configuration, and could not contribute significantly to the ground state. When overlapping regions are encountered the molecule is assigned to

one, and then the other complex. That complex where the common molecule contributes most to the ground state combination retains the molecule for the final energy calculation.

Model characteristics and performance

The MS-EVB2 force field, and consequently the parameterization used for the SCI-MS-EVB force field, was fit¹⁷ to MP2 cc-pVTZ gas phase cluster geometries and formation energies.^{10,11} This parameterization is in excellent agreement with the proton transfer barriers calculated from high level (QCISD(t)/cc-pVTZ) *ab initio* studies²⁰ for the H_5O_2^+ dimer at various O-O distances. The interaction energies and geometrical properties of small clusters are reasonably reproduced, but the model was ultimately developed to model solvation and transport in significantly larger systems. The question is then the performance and characteristics of the model when employed in bulk phase simulations.

As previously discussed, Eigen and Zundel like solvation structures (Figure 1.2) are typically used to describe the solvation state of the excess proton in water. While these structures have been unambiguously identified in gas phase calculations,^{10,11} they are only ideal structures. A range of structures between these two limiting states can be found in the liquid phase, separated by only a very small free energy difference. One useful coordinate for quantifying the continuum of structures is simply the difference between the two largest EVB populations.

This coordinate is exactly zero for the totally symmetric Zundel structure, and otherwise takes on finite values for increasingly Eigen like solvation. Figure 1.4 displays the free energy of the varying configurations as a function of this coordinate. As can be

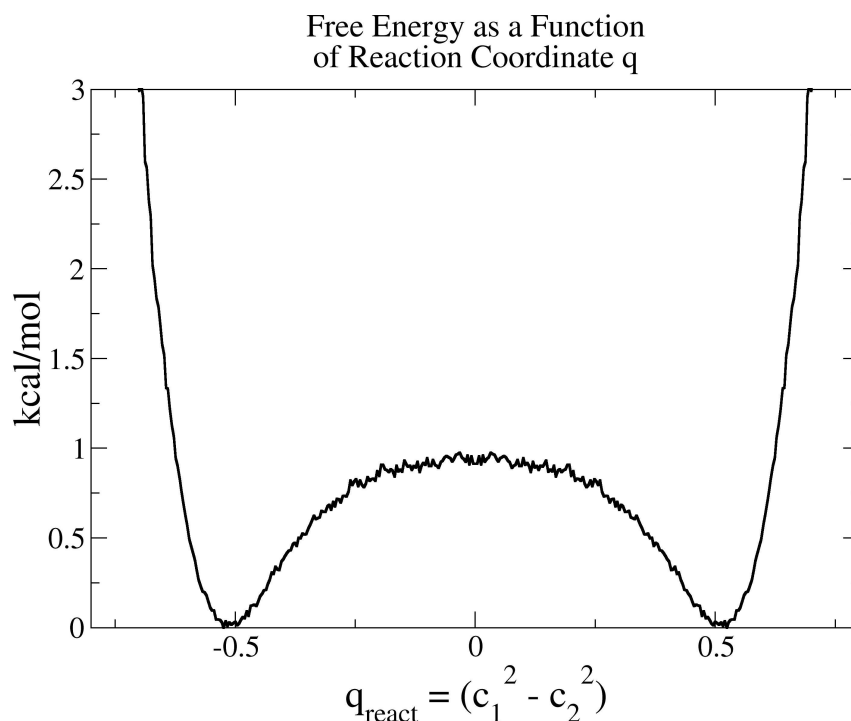


Figure 1.4. Free energy as a function of the difference between the two largest EVB populations.

seen, the free energy barrier between Eigen-to-Eigen transitions is only around 1kcal/mol. One might then suppose that the free energy barrier to the process of bulk phase proton transport is nominally 1kcal/mol.

This, however, assumes that the formation of some Zundel-like intermediate is significantly limiting. The model predicts that solvent rearrangement in the molecules adjacent to the cation limits proton transport.

Day et al.¹⁷ have shown that the Eigen-to-Eigen auto correlation function displays a complicated multiexponential decay similar to that observed for the hydrogen-bond breaking process. Further, Lapid et al.²¹ have demonstrated that the proton transport event is a result of a complicated series of rearrangements within the cation's solvation shells.

And indeed, when compared with experiment, the activation energy computed from temperature dependence of the proton self-diffusion (Figure 1.5) suggests that the MS-EVB2 model accurately reproduces the real-world dynamical rearrangement process.

One might wonder how the proton transfer events contribute, if at all, to the overall diffusion of the excess proton. If the diffusion process is limited by solvent rearrangement around the cation, then perhaps the cation does not diffuse through discrete transport events, but rather through simple vehicular diffusion like any other ion. It is possible to decompose the diffusion of the excess proton into contributions from each of these diffusion mechanisms.

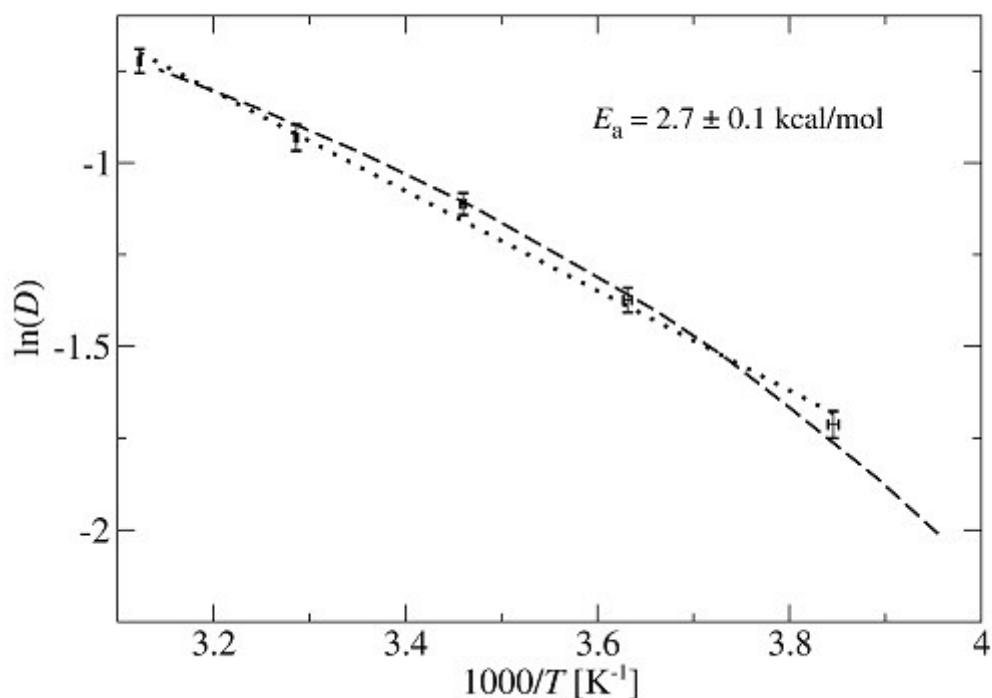


Figure 1.5. The temperature dependent self-diffusion of the excess proton.²¹

As it turns out, proton transfer events are quite significant to the overall diffusion of the excess proton. The displacement vector of the molecule with the largest population can be written as,

$$\vec{r}_{CEC_1}(t) - \vec{r}_{CEC_1}(0) = \Delta \vec{r}_{CEC_1} = \Delta \vec{r}_c + \Delta \vec{r}_d, \quad 1.10$$

so the total displacement is written as the sum of the displacement due to the discrete identity changes of the most populated state and the displacement due to simple continuous Brownian motion respectively. At long times the mean squared displacement (MSD) of the excess protonic charge is nominally the displacement of the largest state. Within this approximation the contribution of the discrete and continuous components can be found by investigating the MSD of the most populated state,

$$\langle \Delta \vec{r}_{CEC_1} \cdot \Delta \vec{r}_{CEC_1} \rangle = \langle \Delta \vec{r}_c \cdot \Delta \vec{r}_c \rangle + \langle \Delta \vec{r}_d \cdot \Delta \vec{r}_d \rangle + 2 \langle \Delta \vec{r}_c \cdot \Delta \vec{r}_d \rangle. \quad 1.11$$

Figure 1.6 shows the MSD for the total displacement and each contributing component. The discrete or Grotthuss component of the total displacement apparently accounts for nearly 2/3 of the total diffusion.

So, we can see that the discrete translocations due to the identity change of the largest population are significant for the diffusion of the excess proton, but are mediated through the dynamics of the hydrogen-bond cleavage of solvent rearrangement.

Significantly more validation of the MS-EVB2 model has been carried out. The following two sections will provide background on the application of the MS-EVB2 and SCI-MS-EVB methods detailed in the following chapters. For a thorough examination of the model and implementation, as well as its use for a variety of systems, see these references^{16-19,21-32} and the references therein.

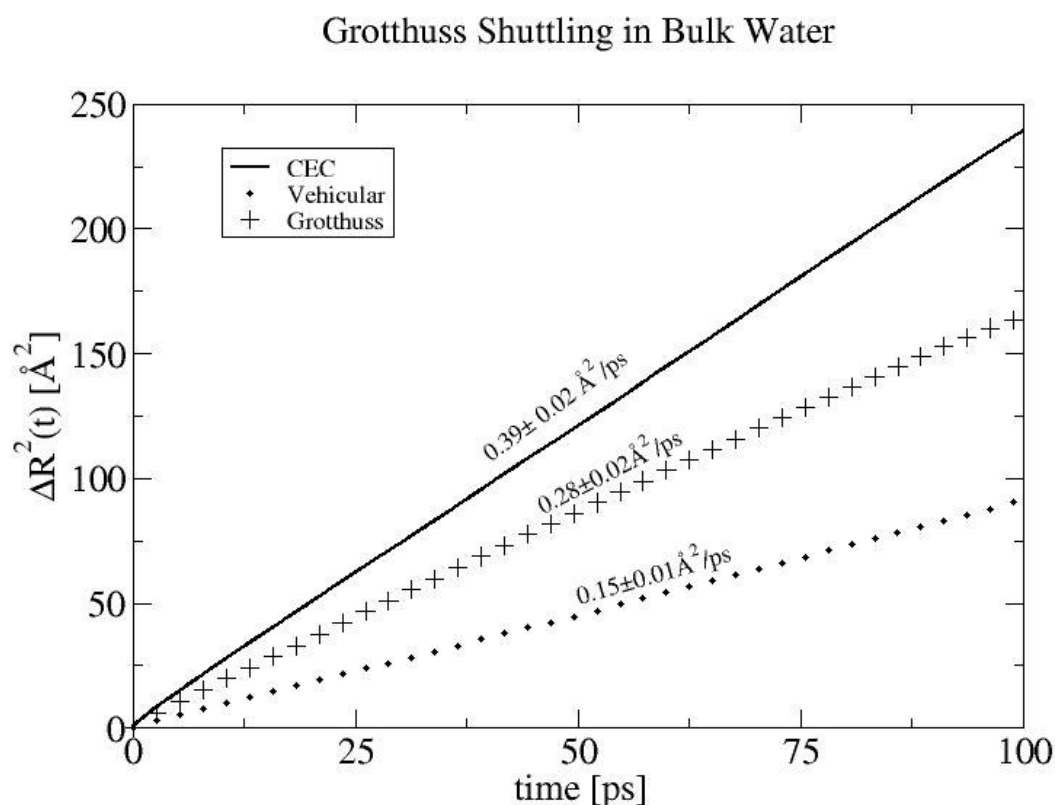


Figure 1.6. The mean squared displacement for the total, discrete, and continuous portions for the excess proton.

Ions at the liquid/vapor interface

The nature of ion solvation near aqueous interfaces is critical in characterizing disparate but fundamental chemical processes. For example, important atmospheric chemical processes are enhanced through surface interactions of ambient gases and NaCl containing aerosols.³³ Production of secondary organic aerosols, suspected to participate in climate forcing processes, has been shown to depend significantly on the acidified surfaces of atmospheric aerosols.³⁴ Likewise, important biological processes are dependent on the interactions of hydrophobic and hydrophilic regions and their mediation

through ionic solvation.³⁵⁻³⁸ And, as unrelated as atmospheric and biological chemistry may appear, it seems that, at least with respect to the phenomena engendered at these boundaries, the two topics have much in common.³⁹

One might intuitively expect ion concentration to be nominally uniform throughout a liquid due to charge repulsion, or perhaps even a marginal deficit at the liquid/ vapor interface due to the incomplete solvation of the ion. This reasoning, however, fails to account for structuring of the liquid through hydrogen bonding and the ordering of the water molecules solvating the ion. The ordering of the water about the ion is dependent on the ionic charge, the size of the ion, and the ionic polarizability.

For example, in a solution of NaCl and water the structure of the Cl⁻ hydration shell has no well-defined symmetry that, unlike the Na⁺ counterion, disrupts the hydrogen bonding of the solvating water molecules into the second solvation shell of the Cl⁻ ion.⁴⁰ There are favorable interactions with the strongly solvating molecules in the first solvation shell, but the disruption of the extended hydrogen bond network through the disordered second solvation shell is unfavorable. The deleterious effects of this disordering are mitigated at the liquid/vapor interface where the second solvation shell can be shed; more so adjacent to curved interfaces.⁴¹

The first experimental evidence for a potential surface enhancement of aqueous ions was indirect, initially presented to explain anomalous experimental results like the uptake of Cl₂ and Br₂ gasses by salt solutions.⁴² Subsequent molecular dynamics simulations supported this proposed surface enhancement, and have further clarified the role of ion charge, size, and polarizability.^{33,43-45} However, simulations present support

for the proposed surface enhancement, but they are sensitive to the ion-water potential interaction.⁴⁶⁻⁴⁸ So certainly, more direct experimental support was needed.

The nonlinear spectroscopic technique sum-frequency vibrational spectroscopy (SFVS) enables the evaluation of the liquid surface of the liquid/vapor interface. While the technique cannot directly probe the concentration of ions, it does directly evaluate the nature of hydrogen bonding at the interface. Investigations using SFVS⁴⁹⁻⁵¹ indicate that anions are present at the interface, and further, leave the hydrogen bonding structure of the interface unchanged, as would be implied by the previously discussed results of Stuart and Berne.⁴¹ So it appears, excluding F^- ,⁵² halide ions in general exhibit surface enhancement while cations exhibit no such preference, albeit forming an anion double layer in deference to the anionic surface enhancement. We know that the nature of proton solvation is fundamentally different than that of other cations.^{8,9} How then does the solvated proton behave near the liquid/vapor interface?

Chapter 2 presents the first publication of a molecular dynamics simulation that provides evidence for surface *enrichment* of the hydrated proton at the liquid vapor interface. Subsequently, Burnham et al.²² have published temperature dependent equilibrium distributions for the $Na^+(H_2O)_{100}$ and $H^+(H_2O)_{100}$ clusters, wherein they report the Na^+ ion showed significant surface residence below the cluster melting temperature and interior solvation above the cluster melting temperature, whereas the solvated proton exhibited significant surface residence for all temperatures. Additionally, recent *ab initio* molecular dynamics simulations have also confirmed this putative surface enrichment of the hydrated proton.^{53,54}

When the excess proton covalently bonds to an adjacent water molecule forming a hydronium ion the oxygen atom of that molecule assumes some of the excess positive charge. This results in the exclusion of a solvating water molecule from the ‘lone pair’ side of the hydronium ion in the first solvation shell. The coordination of the former water molecule is reduced from four solvating water molecules to three strongly solvating molecules and a significant void above the oxygen atom. Analogous to the previously described disruption of the hydrogen bond network in the second solvation shell of the Cl^- ion, the hydronium ion disrupts the hydrogen bond network in the first solvation shell and, likewise, can mitigate this disruption at the liquid/vapor interface. However, unlike the chloride anion, the hydrated proton forms highly symmetric and anisotropic solvation structures.

This anisotropic ordering and enrichment at the liquid/vapor interface is akin to that for the small amphiphile methanol. Computer simulation⁵⁵ and SFSV data⁵⁶ demonstrate a preferential ordering of methanol at the liquid/vapor interface of the neat liquid, such that the methyl groups of those molecules at the surface are directed away from the liquid into the vapor phase. Further, for methanol-water solutions both simulation⁵⁷ and experiment^{58,59} exhibit methanol surface enrichment and the same preferential orientation of the methanol methyl groups.

The similarities between the surface enrichment and preferential orientation of methanol and the solvated proton begs the question; is the hydronium cation an amphiphile like methanol? The natural experiment would be to simulate the hydrated proton in a mixed dielectric distinct from the liquid/vapor or liquid/vacuum interface. Chapter 3 describes simulations of several methanol-water solutions of varying

concentration wherein the solvated proton was found to have a significant anisotropic association with the hydrophobic methanol methyl group,²⁴ further supporting the amphiphilic character of the hydrated proton.

Proton transport in hydrated Nafion

The continued growth of developed and developing nations' economies is largely dependent on world energy supplies.⁶⁰ Increasing demands placed on global energy markets, for example through the current rapid expansion of the Chinese economy,⁶¹ has heightened the already anxious atmosphere surrounding the volatility of conventional energy supplies. This need for inexpensive and reliable domestic energy sources, coupled with the desire to minimize environmental impacts, has motivated significant interest in nonconventional energy conversion and delivery methods. For example, fuel cells, a ~170 year old technology⁶² once relegated to esoteric applications in space and military programs,⁶³ have found their way into commercial electronics and prototype automobiles.

A fuel cell, like a battery, converts chemical energy directly into electrical current. However unlike a battery, the fuel cell does not store the electrochemical energy, but rather the reactants are fed to the cell continuously during operation. Typically hydrogen, or a hydrogen rich compounds, is used as fuel. Often oxygen is used as the oxidant, and as a matter of convenience, can be obtained directly from the air as in air breathing fuel cells.

Nafion

Polymer electrolyte membrane fuel cells (PEMFC) are distinguished by the use of an electrolytic polymer membrane as the separating electrolyte. Of the various polymer electrolyte membranes (PEMs), Du Pont's Nafion is perhaps the most widely studied. Nafion is constructed as a copolymer; a polytetrafluoroethylene (PTFE) backbone supporting several relatively short sulfonate terminated perfluorovinyl ether side-chains (Figure 1.7).

Of the various 'flavors' of Nafion, Nafion 117 is the most widely used formulation. This membrane has a nominal thickness of 0.007 in. and a weight ratio of 1100 g of dry membrane per mole of sulfonate group, or equally, an equivalent weight (EW) of 1100. This weight ratio has also been produced in other thicknesses, i.e., Nafion 115 and Nafion 120. The EW is related to the value of m in Figure 1.7 by $EW = 100m + 446$. So, for an equivalent weight of 1100, m would be around 6.5. It should be noted that the computer simulation literature often confuses Du Pont's labeling scheme and frequently refers to bulk 1100 EW Nafion simply as Nafion 117, an error I have regrettably perpetuated in Chapter 4.

Nafion morphology

The morphological detail of Nafion is broadly characterized by a separation of the

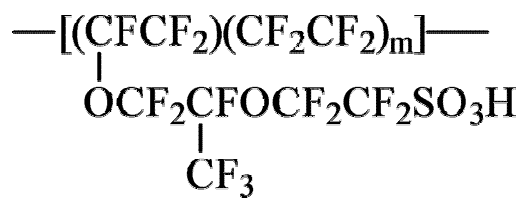


Figure 1.7. The polymeric structure of Nafion.

hydrophobic PTFE and hydrophilic ionic domains. Although the microscopic organization of Nafion has been the focus of significant experimental focus, X-ray^{64,65} and neutron^{66,67} diffraction/scattering in particular, there is still no established detailed morphological model. Proposed morphological models, beginning with the cluster-network model proposed by Gierke et al.,⁶⁸ have included lamellar ordering,⁶⁹ sandwich structure,⁷⁰ rod-like ordered PTFE,⁷¹ to name just a few. However, an essential feature of all plausible models is a local aggregation of sulfonate ions and solvating water.

A great deal of theoretical and computational effort has also been directed at elucidating the characteristics of Nafion. A number of atomistic simulations have been performed.^{25,72-78} Some have attempted to further elucidate the morphological detail of the local hydrophobic/hydrophilic phase separation.^{73,75,76} Regrettably, the relatively short time and length scales available on current computer hardware cast significant doubt on the weight of the conclusions drawn from these atomic simulations. Although well-converged morphological details are lacking in these computer simulations, other significant properties like hydration dependant diffusion⁷³ or preferential cation transport⁷⁴ have been successfully described.

Ion transport

Unlike the morphological details, ion dependant transport⁷⁹ and hydration dependant ionic transport^{79,80} has been well characterized. Of course, as interest in Nafion is almost exclusively as an electrolyte for use in fuel cells, particular attention has been given the acidic form of Nafion.^{81,82} As previously discussed, computational efforts have been particularly successful in describing ion transport. Proton transport rates, in

particular, have been successfully reproduced with statistical mechanical modeling.⁸³⁻⁸⁵

Unfortunately, these models lack any real dynamical insight.

A number of molecular dynamics studies of the acidic form of Nafion have been performed, albeit with severe approximations which disallow some^{77,78} or all^{74,75,86} proton diffusion through the extended hydrogen bond network. It has been shown (Chapter 4)²⁵ that simple nondissociable potentials lead to erroneous dynamics. A complete understanding of molecular scale phenomena is critical for the systematic design of improved PEM for use in PEMFC. Increasing this understanding is the goal of the work presented in Chapters 4 and 5.

References

- (1) Grotthuss, C. J. T. d. *Ann. Chim. (Paris)* **1806**, 58, 54.
- (2) Dalton, J. *A new system of chemical philosophy*; Manchester, 1808.
- (3) Ciccotti, G.; Hoover, W. G. *Molecular dynamics simulations of statistical-mechanical systems*; North-Holland, Amsterdam, 1986.
- (4) Allen, M. P.; Tildesley, D. J. *Computer simulations of liquids*; Oxford, 1987.
- (5) Haile, J. M. *Molecular dynamics simulation*; Wiley, 1992.
- (6) Rapaport, D. C. *The art of molecular dynamics simulation*; Cambridge Univ. Press, 1995.
- (7) Agmon, N. *Chem. Phys. Lett.* **1995**, 244, 456.
- (8) Eigen, M. *Angew. Chem. Int. Edn. Engl.* **1964**, 3, 1.
- (9) Zundel, G. *The hydrogen bond - Recent developments in theory and experiments. II Structure and spectroscopy*; North-Holland, Amsterdam, 1976.
- (10) Ojamae, L.; Shavitt, I.; Singer, S. J. *Int. J. Quantum Chem., Quantum Chem. Symp.* **1995**, 29, 657.

- (11) Ojamae, L.; Shavitt, I.; Singer, S. J. *J. Chem. Phys.* **1998**, *109*, 5547.
- (12) Warshel, A. *Computer modeling of chemical reactions in enzymes and solutions*; Wiley: New York, 1991.
- (13) Mulliken, R. S. *J. Chem. Phys.* **1964**, *61*, 20.
- (14) Coulson, C. A.; Danielsson, U. *Ark. Phys.* **1954**, *8*, 239.
- (15) Lobaugh, J.; Voth, G. A. *J. Chem. Phys.* **1996**, *104*, 2056.
- (16) Schmitt, U. W.; Voth, G. A. *J. Chem. Phys.* **1999**, *111*, 9361.
- (17) Day, T. J. F.; Soudackov, A. V.; Čuma, M.; Schmitt, U. W.; Voth, G. A. *J. Chem. Phys.* **2002**, *117*, 5839.
- (18) Wu, Y.; Voth, G. A. *ms in preparation* **2006**.
- (19) Wang, F.; Voth, G. A. *J. Chem. Phys.* **2005**, *112*, 144105.
- (20) Kochanski, E.; Kelterhaum, R.; Klein, S.; Rohmer, M. M.; Rahmouni, A. *Adv. Quantum Chem.* **1997**, *28*.
- (21) Lapid, H.; Agmon, N.; Petersen, M. K.; Voth, G. A. *J. Chem. Phys.* **2004**, *122*, 014506.
- (22) Burnham, C. J.; Petersen, M. K.; Day, T. J. F.; Iyengar, S. S.; Voth, G. A. *J. Chem. Phys.* **2006**, *124*, 024327.
- (23) Petersen, M. K.; Iyengar, S. S.; Day, T. J. F.; Voth, G. A. *J. Phys. Chem. B* **2004**, *108*, 14804.
- (24) Petersen, M. K.; Voth, G. A. *J. Phys. Chem. B* **2006**, *110*, 7085.
- (25) Petersen, M. K.; Wang, F.; Blake, N. P.; Metiu, H.; Voth, G. A. *J. Phys. Chem. B* **2005**, *109*, 3727.
- (26) Schmitt, U. W.; Voth, G. A. *Chem. Phys. Lett.* **2000**, *36*.
- (27) Smondyrev, A. M.; Voth, G. A. *Biophys. J.* **2002**, *83*, 1987.
- (28) Brewer, M. L.; Schmitt, U. W.; Voth, G. A. *Biophys. J.* **2001**, *80*, 1691.
- (29) Day, T. J. F.; Schmitt, U. W.; Voth, G. A. *J. Am. Chem. Soc.* **2000**, *122*, 12027.

- (30) Kim, J.; Schmitt, U. W.; Gruetzmacher, J. A.; Voth, G. A.; Scherer, N. E. *J. Chem. Phys.* **2002**, *116*, 737.
- (31) Cuma, M.; Schmitt, U. W.; Voth, G. A. *Chem. Phys.* **2000**, 258, 187.
- (32) Cuma, M.; Schmitt, U. W.; Voth, G. A. *J. Phys. Chem. A* **2001**, *105*, 2814.
- (33) Knipping, E. M.; Lakin, M. J.; Foster, K. L.; Jungwirth, P. *Science* **2000**, 288, 301.
- (34) Jang, M.; Czoschke, N. M.; Lee, S.; Kamens, R. M. *Science* **2002**, 298, 814.
- (35) Yaminsky, V.; Ohnishi, S. *Langmuir* **2003**, *19*, 1970.
- (36) Steitz, R.; Gutberlet, T.; Hauss, T.; Klosgen, B.; Krastev, R.; Schemmel, S.; Simonsen, A. C.; Findenegg, G. H. *Langmuir* **2003**, *19*, 2409.
- (37) Jensen, T. R.; Jensen, M. O.; Reitzel, N.; Balashev, K.; Peters, G. H.; Kjaer, K.; Bjornholm, T. *Phys. Rev. Lett.* **2003**, *90*, 086101.
- (38) Lum, K.; Chandler, D.; Weeks, J. D. *J. Phys. Chem. B* **1999**, *103*, 4570.
- (39) Ball, P. *Nature* **2003**, 423, 25.
- (40) Lyubartsev, A. P.; Laaksonen, A. *J. Phys. Chem.* **1996**, *100*, 16410.
- (41) Stuart, S. J.; Berne, B. J. *J. Phys. Chem. A* **1999**, *103*, 10300.
- (42) Hue, J. H.; Shi, Q.; Davidovits, P.; Worsnop, D. R.; Zahniser, M. S.; Kolb, C. E. *J. Chem. Phys.* **1195**, *99*, 8768.
- (43) Jungwirth, P.; Tobias, D. *J. Phys. Chem. B.* **2002**, *106*, 6361.
- (44) Jungwirth, P.; Tobias, D. *J. Phys. Chem. B* **2001**, *105*, 10468.
- (45) Dang, L. X. *J. Chem. Phys.* **1999**, *110*, 1526.
- (46) Perera, L.; Berkowitz, M. L. *J. Chem. Phys.* **1991**, *95*, 1954.
- (47) Carignano, M. A.; Karlström, G.; Linse, P. *J. Phys. Chem. B* **1997**, *101*, 1142.
- (48) Stuart, S. J.; Berne, B. J. *J. Phys. Chem.* **1996**, *100*, 11934.

- (49) Raymond, E. A.; Richmond, G. L. *J. Phys. Chem. B* **2004**, *108*, 5051.
- (50) Liu, D.; Ma, G.; Levering, L. M.; Allen, H. C. *J. Phys. Chem. B* **2004**, *2252*.
- (51) Raymond, E. A.; Tarbuck, T. L.; Brown, M. G.; Richmond, G. L. *J. Phys. Chem. B* **2003**, 546.
- (52) Garrett, B. C. *Science* **2004**, *303*, 1146.
- (53) Iyengar, S. S.; Day, T. J. F.; Voth, G. A. *Int. J. Mass Spec.* **2005**, *241*, 197.
- (54) Iyengar, S. S.; Petersen, M. K.; Day, T. J. F.; Burnham, C. J.; Tiege, V. E.; Voth, G. A. *J. Chem. Phys.* **2005**, *123*, 084309.
- (55) Matsumoto, M.; Kataoka, Y. *J. Chem. Phys.* **1989**, *90*, 2398.
- (56) Superfine, R.; Huang, J. Y.; Shen, Y. R. *Phys. Rev. Lett.* **1991**, *66*, 1066.
- (57) Matsumoto, M.; Takaoka, Y.; Kataoka, Y. *J. Chem. Phys.* **1993**, *98*, 1464.
- (58) Miranda, P. B.; Shen, Y. R. *J. Phys. Chem. B* **1999**, *103*, 3292.
- (59) Raina, G.; Kulkarni, G. U.; Rao, C. N. R. *J. Phys. Chem. A* **2001**, *105*, 10204.
- (60) "World energy and economic outlook," Energy Information Administration, 2005.
- (61) "China Quarterly Update," World Bank Office, Beijing, 2006.
- (62) Bossel, U. *The birth of fuel cell 1835-1845*; European fuel cell forum: Gottingen, 2000.
- (63) Sattler, G. *J. Power Sources* **2000**, *86*, 61.
- (64) Fujimura, M.; Hashimoto, T.; Kawai, H. *Macromolecules* **1981**, *14*, 1309.
- (65) Fujimura, M.; Hashimoto, R.; Kawai, H. *Macromolecules* **1982**, *15*, 136.
- (66) Roche, E. J.; Pineri, M.; Dupelssix, R.; Levelut, A. M. *J. Polym. Sci.* **1981**, *19*, 1.
- (67) Roche, E. J.; Pineri, M.; Dupelssix, R. *J. Polym. Sci.* **1982**, *20*, 107.
- (68) Gierke, T. D.; Munn, G. E.; Wilson, F. C. *J. Polym. Sci.* **1981**, *19*, 1687.

- (69) Litt, M. H. *Polym. Prepr.* **1997**, 38, 80.
- (70) Haubold, H. G.; Vlad, T.; Jungbluth, H.; Hiller, P. *Electrochim. Acta.* **2001**, 46, 1559.
- (71) Rubatat, L.; Rollet, A. L.; Gabel, G.; Diat, O. *Macromolecules* **2002**, 35, 4050.
- (72) Vishnyakov, A.; Neimark, A. V. *J. Phys. Chem. B* **2001**, 105, 7830.
- (73) Vishnyakov, A.; Neimark, A. V. *J. Phys. Chem. B* **2001**, 105, 9586.
- (74) Elliot, J. A.; Hanna, S.; Elliot, A. M. S.; Cooley, G. E. *Phys. Chem. Chem. Phys.* **1999**, 1, 4855.
- (75) Jang, S. S.; Molinero, V.; Cagin, T.; Goddard, W. A. I. *J. Phys. Chem. B* **2004**, 108, 3149.
- (76) Blake, N. P.; Petersen, M. K.; Voth, G. A.; Metiu, H. *J. Phys. Chem. B* **2005**, 109, 24244.
- (77) Spohr, E.; Commer, P.; Kornyshev, A. A. *J. Phys. Chem. B* **2002**, 106, 10560.
- (78) Seeliger, D.; Hartnig, C.; Spohr, E. *Electrochim. Acta.* **2005**, 50, 4234.
- (79) Gavach, C.; Pamboutzoglou, G.; Nedyalkov, M.; Pourcelly, G. *J. Membr. Sci.* **1989**, 45, 37.
- (80) Porcelly, G.; Oikonomou, A.; Gavach, C. *J. Electroanal. Chem.* **1990**, 287, 43.
- (81) Zawodzinski, T. A.; Neeman, M.; Sillerud, L. O.; Gottesfeld, S. *J. Phys. Chem.* **1991**, 95, 6040.
- (82) Zawodzinski, T. A.; Derouin, C.; Radzinsky, S.; Sherman, R. J.; Smith, V. T.; Springer, T. E.; Gottesfeld, S. *J. Electrochem. Soc.* **1993**, 140.
- (83) Eikerling, M.; Kornyshev, A. A.; Kuznetsov, A. M.; Ulstrup, J.; Walbran, S. *J. Phys. Chem. B* **2001**, 104, 3646.
- (84) Paddison, S. J. *J. New Mat. Electrochem. Systems* **2001**, 4, 197.
- (85) Paddison, S. J.; Paul, R.; Zawodzinski, T. A. *J. Chem. Phys.* **2001**, 115, 7753.

(86) Eikerling, M.; Paddison, S. J.; Pratt, L. R.; Zawodzinski, T. A. *Chem. Phys. Lett.* **2003**, 368, 108.